Self-organizing dynamics of coupled map systems

Michał Żochowski*
Department of Molecular and Cellular Physiology, Yale University School of Medicine, New Haven, Connecticut 06511

Larry S. Liebovitch
Center for Complex Systems, T-8 Florida Atlantic University, 777 Glades Road, Boca Raton, Florida 33431
(Received 26 May 1998; revised manuscript received 22 October 1998)

We show that the feedback from the macroscopic dynamics of a system of coupled units can synchronize the dynamics of these units. We studied the dynamics of maps coupled through their variables and control parameters. The feedback adjusted the values of the parameters of each map by using a function that depended on the difference between the Liapunov exponent of each unit and the Liapunov exponent of the mean field of the system. We showed that synchronization of the maps can be achieved under two different conditions: (1) where the maps interact autonomously without a fixed controlling map and (2) where the maps interact nonautomously with a single controlling map with fixed parameters. This method of feedback control may be useful in controlling more general types of parallel distributed systems. [S1063-651X(99)01303-3]

PACS number(s): 05.45.Ra, 64.60.Cn

I. INTRODUCTION

Collective dynamics of self-organizing systems, which are formed as large ensembles of coupled units, have been studied widely (for example, see [1,2] and references therein). One of the major problems in such self-organizing systems is how the dynamics and interactions between many spatially distributed units synchronize to form large-scale spatiotemporal patterns. Such synchronized behavior has been studied in many theoretical systems such as systems of coupled maps, Lorenz equations, oscillators [3,4], coupled laser systems [5] and neural networks [6–8]. Understanding the mechanisms that underlie such synchronization may help to understand the spatiotemporal synchronization that has been found in the sensory cortex [9,10] and olfactory bulb [11]. It has been speculated that the synchronized activity in the brain is related to the binding problem, that is, the linking together of percepts that are processed in different parts of the brain.

These issues of synchronization in spatially distributed systems have been studied in systems of coupled maps which consist of interacting units whose variables are iterated forward in time. These systems were introduced by Kaneko [12,13], and have attracted rapidly growing attention in recent years [14–18]. They can generate spatiotemporal phenomena such as solitons, freezed random configurations, periodic behavior, intermittency, or chaos [19]. They have been used to model spatiotemporal intermittency in Rayleigh-Bénard convection [20] and spiral waves in the Biełousow-Żabotiński reaction [21].

It is not clear, however, how synchronization of systems can be achieved when the dynamical properties of the units in the system are not identical and can adjust in time to accommodate self-organizing processes. We present here a model that shows that coupling the dynamics of a single unit of the system to the mean signal arriving from other units and employing two readout mechanisms on the receiving unit can produce such self-organizing behavior. The first readout mechanism is a fast coupling of the iterates of the receiving unit to the averaged signal coming from other units. It is a fast mechanism because it produces instantaneous changes in the receiving unit based on the spatially averaged activity of the other elements in the system. The second readout mechanism is a much slower mechanism which is designed to integrate, in time, some property of the incoming signal and induce slow changes in the *macroscopic* dynamical properties of the receiving element. The interaction of these two mechanisms produces self-organization in the coupled system.

The results presented in our paper can be used in information theory and also may have an application in modeling brain function. In the brain it is found [22] that the activity of the neurons maybe modulated by slower acting channels and resulting ion density within a cell (for example, metabathiphic receptors or by altering the Ca^{2+} concentration that regulates ion channel activity). This would correspond to implementation of the slow readout mechanism. Changes in ion concentrations on a large time scale (of the order of tens or hundreds of milliseconds) may lead to changes in dynamical properties of the cells and thus to a changed pattern of neuronal spike firing—the short time scale (of the order of milliseconds) dynamics. The fast readout mechanism can be viewed as implemented by the channels reacting rapidly to the release on a neurotransmitter on the synapse and thus producing fast changes in the postsynaptic potential. Examples of such channels are acetylcholine receptors, which produce rapid influx of Na^{+} ions during depolarization, or GABA receptors, which produce influx of Cl^{-} during the hyperpolarization. The interactions of the action potentials may in turn lead to the formation of the synchronized activity of the firing of many neurons.

The system studied here consists of logistic maps. In terms of coupled maps, the dynamical properties of each unit depend on a parameter, which may be different for different

*Permanent address: Centrum Fizyki Teoretycznej PAN, Al. Lotników 32/46, 02-784 Warsaw, Poland.

units. The question then becomes, how can the parameters of these units be equalized to produce the same dynamical behavior? Depending on the value of the parameter, the dynamics of one map may be periodic, whereas the dynamics of the other map may be chaotic.

The maps were coupled together by having the variables of one map depend on the variables of the other maps. The iterations of the maps and the dependency of the variables of each map on the other maps form the fast time scale in this system. We additionally coupled the maps by having the parameter of each map depend on a function of the variables of the other maps. We determined the changes in the value of the parameter of each map by computing the difference between the Liapunov exponent estimated from the iteration in time of that map and the Liapunov exponent estimated from the average of the variables of the other maps iterated in time. Essentially, this means that the dynamics of each map, as determined by its parameter, is controlled by the macroscopic dynamical properties of the other maps, which is evaluated from their signal. This defines a slower time scale at which the characteristic of each map responds to the overall dynamics of the system. It is worth stressing that in this system units are coupled effectively by one coupling which transmits the value of the iterate at given time step. The unit at the receiving end integrates different properties of that signal over different time scales and incorporates it into two different driving mechanisms.

We studied the synchronization produced by this coupling in (1) a system with autonomously interacting maps without a fixed controlling map and (2) a system with nonautomously interacting maps driven by a controlling map with fixed parameters. In both cases, even though the units start with different dynamical properties, as determined by their parameters (ranging from periodic to chaotic), these systems reach stable synchronized patterns. In the second case, the controlling map can also determine the properties of the pattern.

Controlling the dynamics of a chaotic system is presently a very active line of research and has wide applications in different branches of science. Ott, Grebogi, and Yorke (OGY) [23] showed how one can achieve chaotic control by using a feedback mechanism acting on the control parameters of the system. Other aspects of control were studied earlier in low-dimensional systems [24–26], where the perturbed system is driven to a fixed-point orbit. Since the maps to be controlled can have chaotic dynamics, the work presented here provides a new approach to controlling a chaotic system.

In our previous work [27] we studied how synchronization depends on the feedback between the variables and the parameters of the units and showed how one map can be used to control another map [27]. We now extend that method of control to many interacting maps.

II. DESCRIPTION OF THE MODEL

The system we studied consists of $N=50$ units, each of which is a logistic map. The dynamical properties of each map are determined by its parameter $r^{(i)}$, which initially may be different for each map i. The variable of each map $x^{(i)}$ is iterated forward to time step $n+1$ by

$$x_{n+1}^{(i)}=f_i(r_n^{(i)},x_n^{(i)})=r_n^{(i)}x_n^{(i)}(1-x_n^{(i)}), \tag{1}$$

where $x\in[0,1]$ and $r\in[0,4]$.

The motivation for the following coupling is to make the dynamics of each map depend on its internal dynamics and on the input from the average state of the rest of the maps:

$$x_{n+1}^{(i)}=\frac{f_i(r_n^{(i)},x_n^{(i)})+[\alpha_1/(N-1)]\sum_{j,j\neq i} f_j(r_n^{(j)},x_n^{(j)})}{1+\alpha_1}, \tag{2}$$

where α_1 indicates the strength of the interaction between each map and the rest of the system, which is the same for all the maps; the simulations described in the next section were performed for $\alpha_1=0.6$.

The state of the map in the next time step is thus dependent on its previous state and the average state of the rest of the maps. The value of the iterate at the given site is then normalized not to exceed 1. Single units act here as an integrator of the dynamics of whole system, and its evolution is a function of its own state and the state of other elements of the system. This maybe viewed as an approximation of a neuron, where the cell acts as an integrator of the depolarizing and hyperpolarizing changes in potential, which are due to changes in ionic density.

We will show that when the parameter of a single map is coupled to the difference of the estimated Liapunov exponents between the mean field of the variables of other maps and the map itself, the maps can adjust their parameters and then fully synchronize.

The two variables $r_n^{(j)}$ and $x_n^{(j)}$ evolve at different time scales. The parameters $r_n^{(j)}$ evolve much slower than the variables $x_n^{(j)}$. The Liapunov exponents computed from each map and the mean field depend primarily on $x_n^{(j)}$. Thus, the slowly varying value of r does not effect the computation of the Liapunov exponents.

The Liapunov exponent for each map is computed from the iterations of that map $\tilde{x}^{(s)}$ uncoupled from the other maps. That is, it is based on the evolution of

$$\tilde{x}_{n+1}^{(s)}=r_n^{(s)}x_n^{(s)}(1-x_n^{(s)}). \tag{3}$$

The Liapunov exponent is given by

$$\lambda^{(s)(i)}=\lim_{N\to\infty}\frac{1}{N}\sum_{j=1}^{N}\ln\left|\frac{df_i}{dx}(\overline{r^{(i)}},\tilde{x}_j^{(i)})\right|. \tag{4}$$

The mean field $h_{n+1}^{(i)}$ at time step n is given by

$$h_n^{(i)}=\frac{1}{N-1}\sum_{j,j\neq i} f_j(r_n^{(j)},x_n^{(j)}). \tag{5}$$

The Liapunov exponent for the mean field is given by

$$\lambda^{(mf)(i)}=\lim_{N\to\infty}\frac{1}{N}\sum_{j=1}^{N}\ln\left|\frac{df_i}{dx}(\overline{r^{(i)}},h_j^{(i)})\right|. \tag{6}$$

We approximate the Liapunov exponents for each map and the mean field by using the running sum

$$\lambda_{n+1}^{(i)} = \frac{\lambda_n^{(i)} + \alpha_2 \ln|df_i/dx|}{1+\alpha_2}. \tag{7}$$

$\alpha_2 = 0.02$ was set during the simulations. We then define the function A used to control the dynamics of r as

$$A(\lambda_n^{(s)(i)}, \lambda_n^{(mf)(i)}) = (|\lambda_n^{(s)(i)} - \lambda_n^{(mf)(i)}|)^{1/4} \times \mathrm{sgn}(\lambda_n^{(s)(i)} - \lambda_n^{(mf)(i)}). \tag{8}$$

The function $A(\lambda_n^{(s)(i)}, \lambda_n^{(mf)(i)})$ could have different forms. We chose the shape of this function to ensure that there are large changes in A for small differences between $\lambda_n^{(s)}$ and $\lambda_n^{(mf)}$ and small changes in A for large differences between $\lambda_n^{(s)}$ and $\lambda_n^{(mf)}$. This ensures that the parameters of the map change when the map is not synchronized to the mean field, but the changes are kept small when it is too far out of synchronization to prevent excessive overshooting of the parameter required for synchronization.

The control method adjusts the parameter of each map by the following:

$$r_{n+1}^{(i)} = r_n^{(i)} + \gamma A(\lambda_n^{(s)(i)}, \lambda_n^{(mf)(i)}), \tag{9}$$

where γ is a constant much less than unity. During the simulations $\gamma = 0.000\,04$.

Additionally, when the parameter of any element increased to the value $r^{(i)} \geqslant 4.0$ it was reinjected at the low end value of $r^{(i)} = 3.1$, and conversely, if the parameter of any element decreased $r^{(i)} \leqslant 3.0$, it was reinjected at the value of $r^{(i)} = 3.98$.

This definition of fast and slow detection mechanisms in the system allows a large separation of the time scales. The first mechanism is an instantaneous reaction of a given unit to the actions of the others. The second one acts as a temporal integrator of the dynamical properties of the system. Thus the same signal integrated on different time scales can act as a driving signal and as a control mechanism.

III. RESULTS

We studied the behavior of this system for two cases: (1) autonomously interacting maps without a fixed controlling map and (2) nonautonomously interacting maps driven by one controlling map with fixed parameters. In both cases, even though the maps start with different parameters and thus different dynamical properties (ranging from periodic to chaotic), the maps reach stable synchronized patterns. In the second case, the controlling map determined the properties of the pattern.

A. Autonomously interacting maps

In the first set of simulations, there were 50 maps coupled to each other, but no controlling map with fixed parameters. The initial values of the variables and parameters were chosen from a uniform distribution over their ranges. Figure 1 shows the evolution of the mean value of the parameters of all the maps. This mean value fluctuated at the beginning and then changed slowly over time. The fluctuations in the pattern were measured by S_n, the standard deviation from the mean value of the averaged iterate.

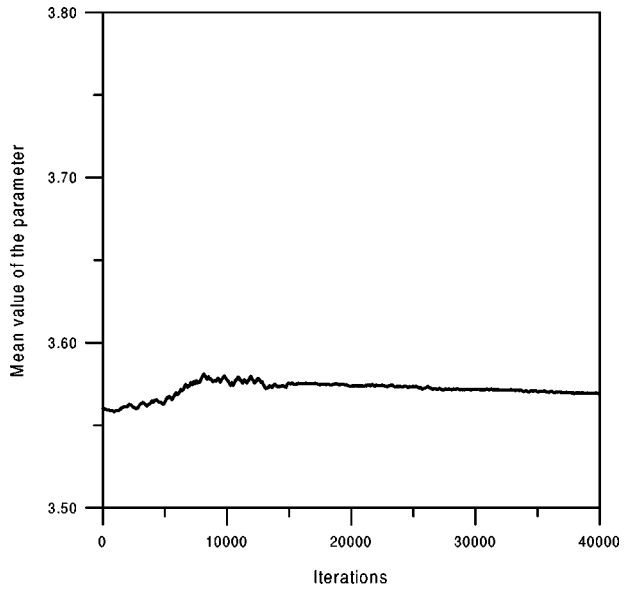

FIG. 1. Autonomous coupled maps (without a controlling map). Evolution in time of the mean value of the parameters of the maps. As the (50) maps synchronize, the mean value stabilizes and then drifts only slowly over time. The initial values of the iterates and parameters were picked at random, $\alpha_1 = 0.6$, $\alpha_2 = 0.02$, $\gamma = 0.000\,04$.

Figure 2 shows that S_n decreased rapidly in time, indicating that the maps quickly evolved toward a synchronized state. Thus, when there is no external control, the maps converged to the averaged dynamical state of the system as a whole.

We also tested the behavior of the model adding different amounts of noise into the system. The equations took the form

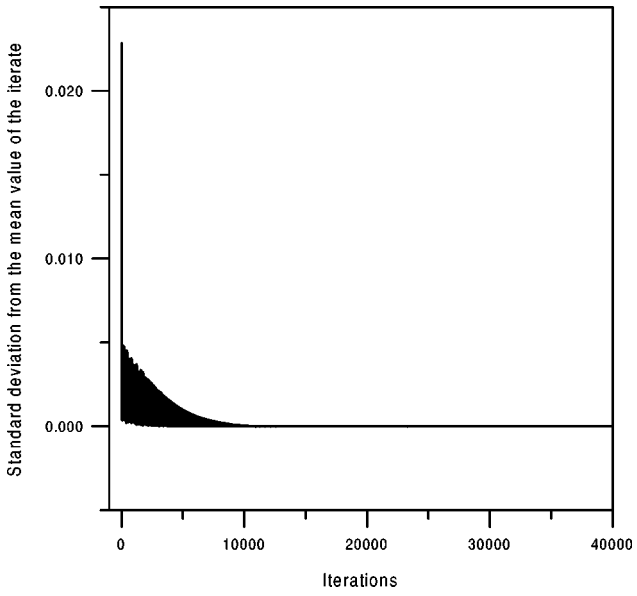

FIG. 2. Autonomous coupled maps (without a controlling map). Evolution in time of the standard deviation from the mean value of the iterate. The difference decreases rapidly in time indicating that the maps quickly evolve toward synchronized behavior. These results are recorded from the same trial as Fig. 1.

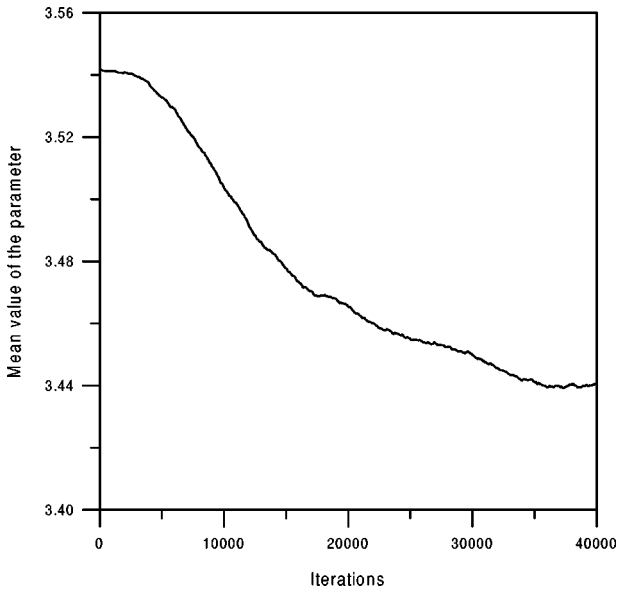

FIG. 3. Behavior of the autonomous maps in the presence of noise. The evolution of the mean value of the parameter is presented. The system is dominated by noise and the parameter stabilizes at the periodic/chaotic transition point. The transition point is lower than for noiseless system as expected. The amplitude of noise, $a_{\text{noise}}=0.01$. Other parameters are as in Fig. 1.

$$x_{n+1}^{(i)}=\frac{f_i(r_n^{(i)},x_n^{(i)})+[\alpha_1/(N-1)]\sum_{j,j\neq i} f_j(r_n^{(j)},x_n^{(j)})+\varepsilon_j}{1+\alpha_1}, \tag{10}$$

where ε_i are random variables. This way of incorporating noise in the system should be viewed as noise in coupling between the units, rather then as noise in the units themselves. These results are presented in Figs. 3 and 4. The

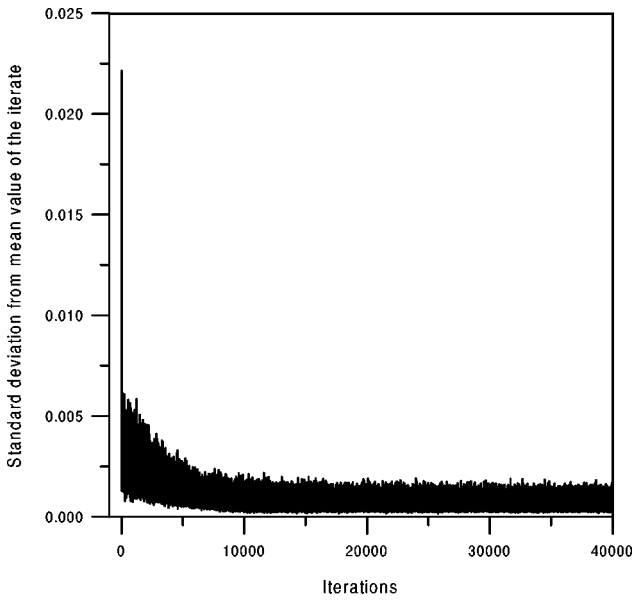

FIG. 4. Behavior of the autonomous maps in the presence of noise. Presents the evolution of standard deviation from the mean value of the iterate. The elements do not synchronize fully. These results are recorded from the same trial as Fig. 3.

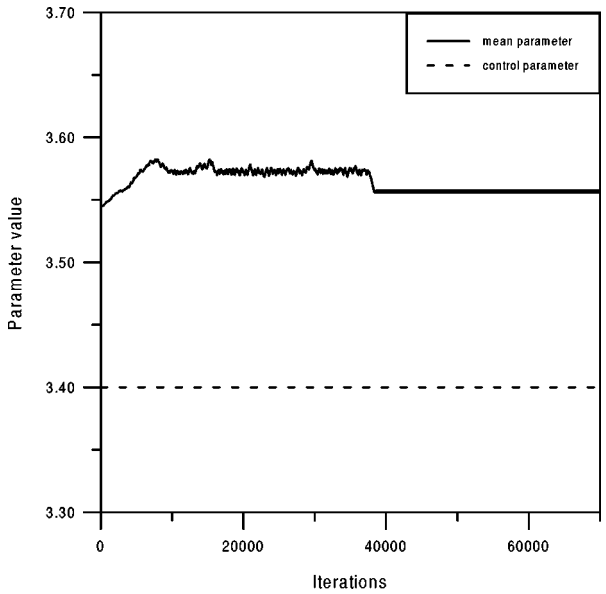

FIG. 5. Nonautonomous coupled maps with one controlling map with fixed parameter $r^{(c)}=3.4$. Evolution in time of the mean value of the parameters of the maps. The parameter converges to the chaotic/periodic dynamics transition point. $\alpha_1=0.6$, $\gamma=0.000\,04$.

degree of synchronization is less with a higher amplitude of noise. With the addition of noise, the system tends to synchronize on a less complex trajectory (one with the smaller Liapunov exponent). When the noise level is high (noise amplitude $a_{\text{noise}}=0.01$) the system always stabilizes at the transition point from periodic to chaotic regime. This is due to the fact that for $a_{\text{noise}}=0.01$ the system dynamics starts to be dominated by noise and the Liapunov exponent tends to zero, which is the value at the transition point.

B. Nonautonomously interacting maps driven by one controlling map

In the second set of simulations, there were 50 maps coupled to each other and to one control map with a fixed parameter. The initial values of the variables and parameters (of the autonomous maps) were again chosen at random from a uniform distribution over their ranges. The control map represents a stable external input or forcing into the system. These simulations explored the ability of the controlling map to synchronize the dynamics of the entire system on a specific trajectory. We found that the controlling map could synchronize the system only over certain ranges of its parameter and that this control was also sometimes intermittent.

When the parameter value of the control maps is set below the value that defines transition from periodic to chaotic behavior $r_{(c)}<3.56$ the maps with unconstrained behavior can synchronize between themselves but cannot synchronize with the control map. Those results are presented for the case when $r_{(c)}=3.4$ in Figs. 5 and 6. Figure 5 presents the evolution of mean value of the parameter, while Fig. 6 shows the changes of standard deviation from the mean value of the iterates. The mean value of the parameter of the unconstrained maps stabilizes around the periodic/chaotic regime transition point. This is due to the fact that below the transition value the Liapunov exponent stops being a monotonic function of the parameter ($r^{(i)}$) for the elements. The above-

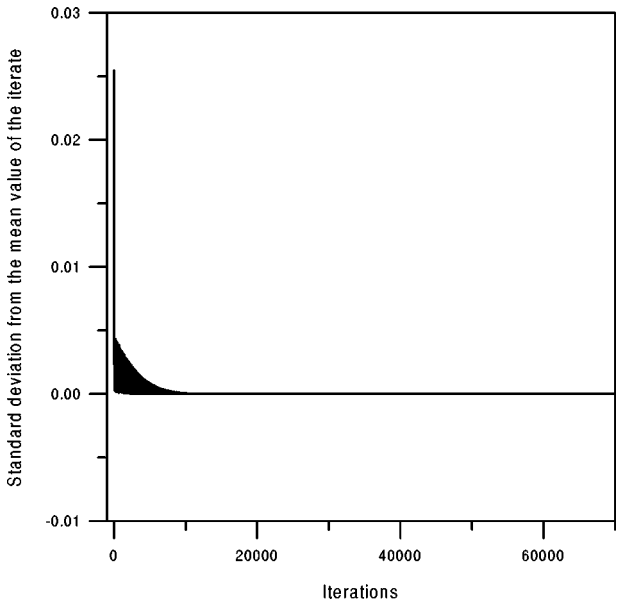

FIG. 6. Nonautonomous coupled maps with one controlling map with fixed parameter $r^{(c)}=3.4$. Evolution of the standard deviation from the mean value of the iterate. The standard deviation tends to zero—the maps synchronize. These results are recorded from the same trial as Fig. 5.

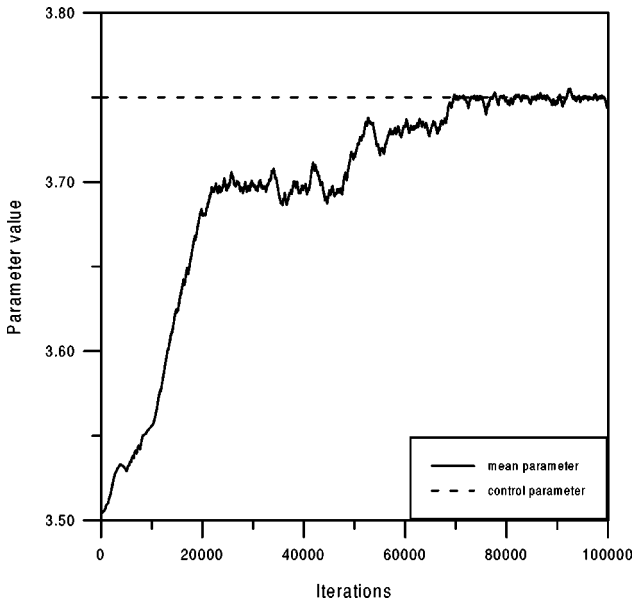

FIG. 7. Nonautonomous coupled maps with one controlling map with fixed parameter $r^{(c)}=3.75$. Evolution in time of the mean value of the parameters of the maps. The mean value of the parameter converges to that of the control map. $\alpha_1=0.6$, $\gamma=0.000\,04$.

mentioned limit applies, however, only to the values of the parameter of the control map. The parameter values for unconstrained maps can take any value. Within the periodic regime the largest value of the Liapunov exponent takes the value of zero at the bifurcation points which is smaller than any positive value of the exponent in the chaotic regimes. Thus the control scheme is working properly.

When the parameter of the control map was larger than the transition value and below $r_{(c)}\leqslant 3.76$, the maps synchronized with each other, adjusted their parameter values to the control map, and synchronized with it. Figure 7 shows results of the simulation for this case. The value of the control parameter was set to $r_{(c)}=3.75$. The mean value of the parameters of the maps approached a nearly constant value equal to that of the parameter of the control map. Figure 8 shows that the standard deviation decreased rapidly in time, indicating that the maps are synchronized.

The parameter range for which system could be effectively controlled and synchronized depended on the value of γ—the constant determining the size of the changes of $r^{(i)}$. With a smaller gamma the mean value of the parameter of autonomous maps converged slower to $r_{(c)}$, but the range of the values for which it converged was substantially increased. Figure 9 presents the evolution of the mean parameter for three different values of γ. The parameter value of the control map was set to $r_{(c)}=3.65$. For $\gamma=0.000\,04$ the system converges to the value of the control parameter. For $\gamma=0.0004$ the system also converges to the value of the control parameter but fluctuates around it noticeably. For $\gamma=0.004$ the system does not converge and stabilizes at some random value. This maybe due to the fact that the control parameter is overshot for many elements repeatedly, and also to the fact that the approximation of the Liapunov exponent may start to fail due to the faster changes in the parameter value.

We also tested whether the model can adjust its final state to the changes in the external stimulus. Those changes were induced by changing the parameter value of the control map during the simulation. The parameter of the control map was changed every 30 000 iterations from $r_{(c)}=3.6$ to $r_{(c)}=3.75$ with a step of 0.05. The system follows the changes of the parameter the control map. The convergence, however, becomes slower with larger values of the control parameter (Fig. 10). As the parameter of the control map

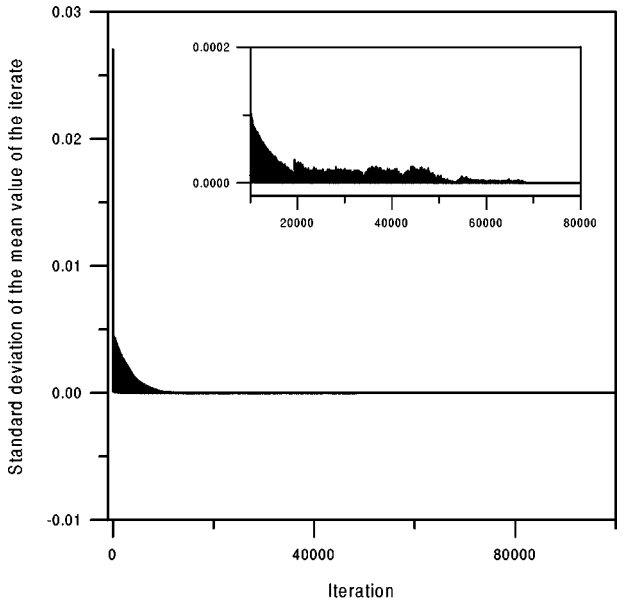

FIG. 8. Nonautonomous coupled maps with one controlling map with fixed parameter $r^{(c)}=3.75$. Evolution of the standard deviation from the mean value of the iterate. The standard deviation tends to zero—the maps synchronize. These results are recorded from the same trial as Fig. 7. The inset magnifies the part of the main picture. $\alpha_1=0.6$, $\gamma=0.000\,04$.

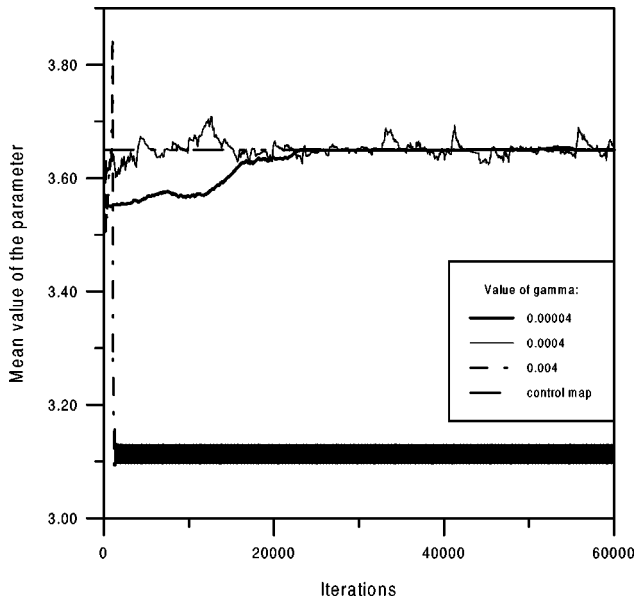

FIG. 9. Nonautonomous coupled maps with one controlling map, $r^{(c)}=3.65$. The value of γ was varied. For smaller values of γ the system converges to the value of the control parameter of the controlling map. For larger values of γ the mean parameter starts to oscillate about the control value. For $\gamma=0.004$ the system fails to stabilize; the units are not synchronized.

changes the units desynchronize briefly but then quickly synchronize again (Fig. 11). This process is slower for the last two cases. This is actually the cause of the slower convergence of the parameter.

When the parameters of the control map were larger, and the dynamics of the control map was more irregular, the

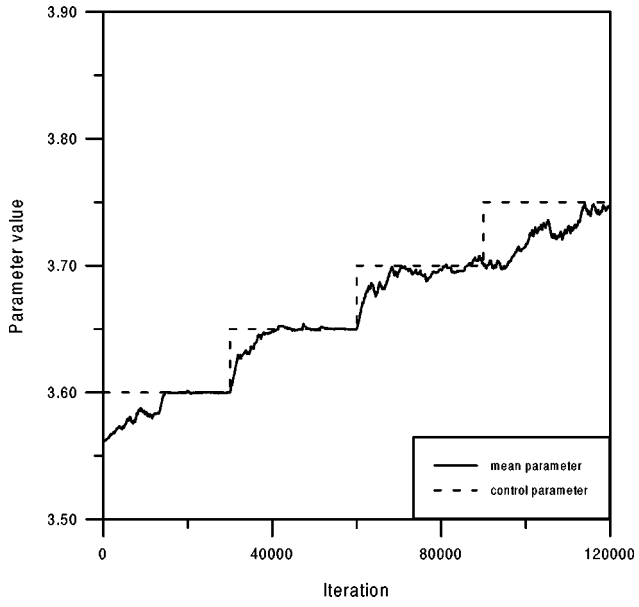

FIG. 10. Nonautonomous coupled maps with one controlling map. Evolution in time of the mean value of the parameters of the maps. The mean value of the parameter converges to that of the control map. The parameter was changed every 30 000 iterations from $r_{(c)}=3.6$ to $r_{(c)}=3.75$ with a step of 0.05. The system follows the changes of the parameter of the control map. $\alpha_1=0.6$, $\gamma=0.000\,04$.

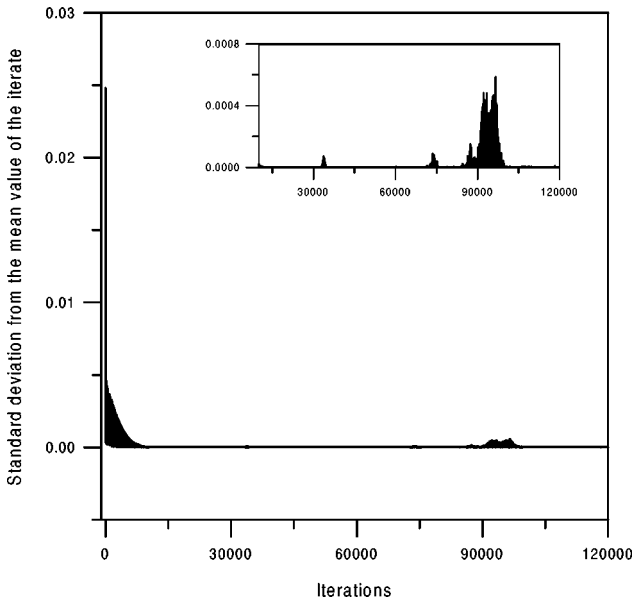

FIG. 11. Nonautonomous coupled maps with one controlling map. Evolution of the standard deviation from the mean value of the iterate. As the parameter of the control map changes the units desynchronize briefly but then synchronize again. These results are recorded from the same trial as Fig. 10. The inset magnifies the part of the main picture. $\alpha_1=0.6$, $\gamma=0.000\,04$.

system was less synchronized and intermittently escaped from the control. This is illustrated for the case when the parameter of the control map was $r=3.91$. Figure 12 shows the larger variation in the mean value of the parameters of the maps. It also shows the evolution of the standard deviation from the mean value of the parameter. As can be seen, the fluctuations in the standard deviation determine the value of the mean parameter. The larger the standard deviation, the lower is the value of the mean value of the parameter. This is due to the fact that the mean signal arriving at the driven site becomes distorted and the fine dynamical structure of the

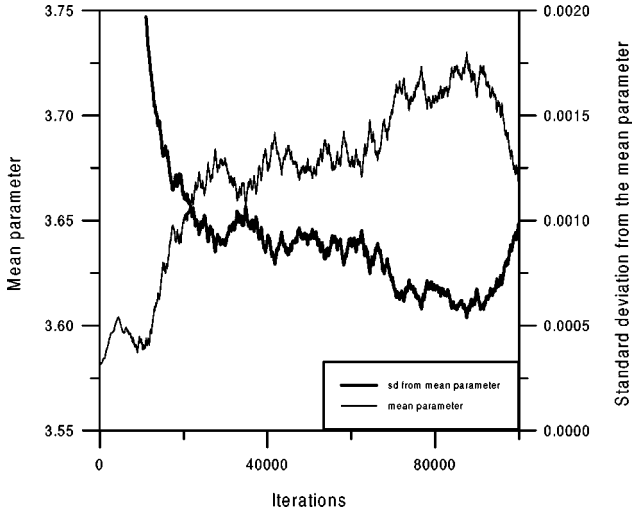

FIG. 12. Nonautonomous coupled maps with one controlling map, $r^{(c)}=3.91$. The system is not able to adjust the parameter and synchronize with the control map. The mean value of parameter oscillates well below the transition point. The oscillations of the mean value of the parameter, however, are highly correlated with the changes in the standard deviation from it.

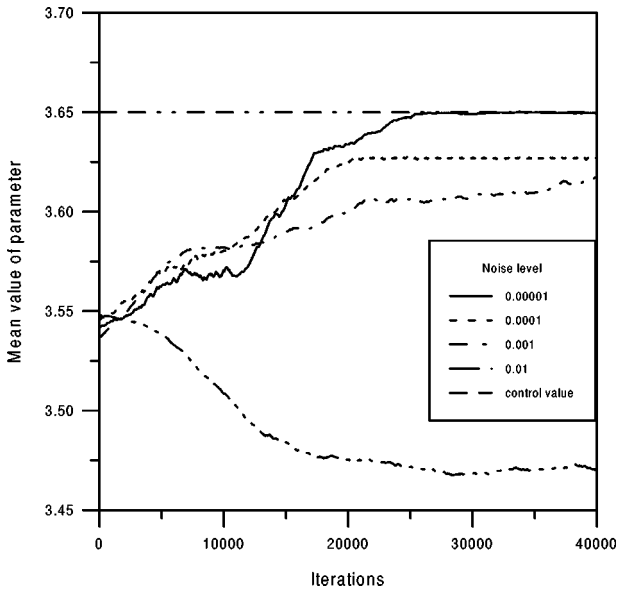

FIG. 13. Nonautonomous coupled maps with one controlling map in the presence of noise, $r^{(c)}=3.65$. Evolution in time of the mean value of the parameters of the maps. The noise level was varied between 0.01 and 0.000 01. The steps were equal to one order of magnitude. The synchronization of the system deteriorates with the increasing noise. For a high noise level $a_{\text{noise}}=0.01$ the system is overridden by noise and the parameter converges to the period ic/chaotic dynamics transition point. $\alpha_1=0.6$, $\alpha_2=0.02$, $\gamma=0.000\,04$.

signal becomes lost. The signal becomes noisy and the value of the Liapunov exponent decreases toward zero.

We also studied the behavior of the model in the presence of noise. Those results are presented in Fig. 13. With the lower amount of noise the maps are able to synchronize but underestimate the Liapunov exponent and the parameter. When the noise level is large ($a_{\text{noise}}=0.01$) the maps fail to fully synchronize and the parameter stabilizes around the transition point from periodic to chaotic behavior. The value of the parameter at this point is shifted and is smaller than for the case without noise. Those results are in agreement with the results obtained earlier for the behavior of single logistic maps in the presence of noise, which shows that the periodic/chaotic transition takes place for lower values of the parameter (see [28]).

IV. CONCLUSIONS

We showed that incorporation of two readout mechanisms applied locally on the post-connection element and acting on two different time scales leads to an adjustment of element properties and global synchronization in a coupled system.

In the example presented here, maps with different dynamical behavior resulting from different initial parameters can synchronize to a state where the variables and parameters of each map are similar. This occurred when the changes in the parameters of the maps were driven by the mean field behavior of the rest of the system. The units of the system were coupled by a single coupling, via their iterates, but employed two readout mechanisms. The first one was a fast readout and it coupled directly, without delay, the iterates of the maps. The second one was a slow readout which coupled the temporal average of a macroscopic property of the signal (the estimated value of the Liapunov exponents) to the map's parameter which in turn controlled the macroscopic behavior of the map.

This synchronization occurred in autonomous systems where the maps are only coupled to each other, as well as nonautonomous systems where the maps are also driven by a central controlling map with fixed parameters. In the first case the dynamics of the system stabilizes on the trajectory determined by the averaged value of the parameter of all the units. In the second case of nonautonomous maps we showed that the system can be effectively controlled by a single element. The degree of control depends on the parameters and thus the dynamical properties of the controlling map. For some ranges of the parameter of the controlling map the entire system is strongly synchronized and for other range the entire system is intermittently synchronized. The system cannot adjust its parameter to that of the control map if the parameter of that map is in the periodic regime. This is due to the fact that the macroscopic dynamical properties (measured here by the estimated Liapunov exponent) stop being a monotonic function of the parameter in the periodic regime.

This mechanism of control, where the parameters of units are adjusted by a function that depends on the difference between the Liapunov exponent of each unit and the Liapunov exponent of the mean field of the system, may also have applications to achieving synchronized control in more general classes of parallel, distributed systems.

This scheme of control and synchronize maybe widely used in information theory and in any other systems that are built of units that can adjust their dynamical properties to code or decode a pattern. A similar mechanism also may play a role in brain function where it is known that changes in cell properties can take place on different time scales. In neurobiology a different readout mechanism can be implemented by activation of different ion channels and changes in ion concentrations. It remains to be seen whether and to what extent biology takes advantage of such mechanisms.

ACKNOWLEDGMENTS

M.Z. wants to thank L. B. Cohen for his comments on the manuscript. This work was supported in part by NIH Grant Nos. EY6234 and NS08437.

[1] M. G. Rosenblum, A. Pikovsky, and J. Kurths, Phys. Rev. Lett. **78**, 4193 (1997).

[2] S. Venkataramani and E. Ott, Phys. Rev. Lett. **80**, 3495 (1998).

[3] J. Kowalski, G. Albert, and G. Gross, Phys. Rev. A **42**, 6260 (1990).

[4] L. Kocarec and U. Parlitz, Phys. Rev. Lett. **77**, 2206 (1996).

[5] H. Winful and L. Rahman, Phys. Rev. Lett. **65**, 1575 (1990).
[6] J. A. J. E. Moreira and F. W. S. Lima, Phys. Rev. E **52**, R2129 (1995).
[7] D. Hansel and H. Sompolinsky, Phys. Rev. Lett. **68**, 718 (1992).
[8] D. Hansel and H. Sompolinsky, J. Comp. Neurosci. **3**, 7 (1996).
[9] J. Prechtl *et al.*, Proc. Natl. Acad. Sci. USA **94**, 7621 (1997).
[10] R. Eckhorn *et al.*, Biol. Cybern. **60**, 121 (1988).
[11] Y. Lam, L. Cohen, and M. Zochowski (unpublished).
[12] K. Kaneko, Prog. Theor. Phys. **72**, 480 (1984).
[13] K. Kaneko, Phys. Lett. A **170**, 210 (1992).
[14] F. Xie and H. Cerdeira, Phys. Rev. E **54**, 3235 (1996).
[15] F. Xie, G. Hu, and Z. Qu, Phys. Rev. E **52**, R1265 (1995).
[16] Y. Nagai, X. Hua, and Y. Lai, Phys. Rev. E **54**, 1190 (1996).
[17] G. Hu, F. Xie, Z. Qu, and F. Zhang, Phys. Rev. E **54**, 1305 (1996).
[18] V. Belykh and E. Mosekilde, Phys. Rev. E **54**, 3196 (1996).
[19] J. Crutchfield and K. Kaneko, in *Directions in Chaos*, edited by H.-B. Lin (World Scientific, Singapore, 1987).
[20] S. Ciliberto and P. Bigazzi, Phys. Rev. Lett. **60**, 286 (1988).
[21] D. Barkley, in *Nonlinear Structures in Dynamical Systems*, edited by L. Lam and H. Noris (Springer-Verlag, New York, 1990).
[22] J. Nicholls, A. Martin, and B. Wallace, *From Neuron to Brain* (Sinauer Associates, Suderland, MA, 1992).
[23] E. Ott, C. Grebogi, and J. Yorke, Phys. Rev. Lett. **64**, 1196 (1990).
[24] B. Huberman and E. Lumer, IEEE Trans. Circuits Syst. **37**, 547 (1990).
[25] S. Sinha, Phys. Lett. A **156**, 475 (1991).
[26] S. Sinha and R. Ramaswamy, Physica D **43**, 118 (1990).
[27] M. Zochowski and L. Liebovitch, Phys. Rev. E **56**, 3701 (1997).
[28] H. G. Schuster, *Deterministic Chaos* (Physik-Verlag GmbH, Weinheim, 1984).